Available online at www.sciencedirect.com
ScienceDirect
European Journal of Medicinal Chemistry 43 (2008) 2840–2852
EUROPEAN JOURNAL OF MEDICINAL CHEMISTRY
http://www.elsevier.com/locate/ejmech

Original article

Pharmacophore based discovery of potential antimalarial agent targeting haem detoxification pathway

Badri Narayan Acharya, Deepika Saraswat, Mahabir Parshad Kaushik*

Discovery Centre, Defence Research and Development Establishment, Jhansi Road, Gwalior, Madhya Pradesh 474002, India

Received 27 November 2007; received in revised form 5 February 2008; accepted 7 February 2008
Available online 4 March 2008

Abstract

Pharmacophore hypotheses were generated from molecules having putative antimalarial activities targeting haem detoxification pathway of malarial parasite. A training set consisting of 33 compounds, whose activities were evaluated for haem polymerization inhibition and against chloroquine resistant (K1) strain of *Plasmodium falciparum*, was optimized to generate hypotheses. The hypothesis showing optimum correlation between actual and estimated activities was validated by Fischer's randomization test at 95% confidence level and used as a model to screen our in-house compound database. Nicotinic acid [*trans*-3-(4-ethoxy-3-methoxy-phenyl)-1-(4-hydroxy-phenyl)-allylidene]-hydrazide (**ALH5**) was obtained as a hit. The compound was synthesized and evaluated against chloroquine sensitive (MRC-02) and resistant (RKL9) strains of malarial parasite *P. falciparum*. The compound showed antimalarial activity in nanomolar range and was found comparable with chloroquine.

Keywords: Malaria; *Plasmodium falciparum*; Haem detoxification; Pharmacophore; Predictive model; Hydrazide

1. Introduction

Malaria is a major health problem in today's world, with 200–500 million clinical cases and two million deaths occurring each year [1]. The development of drug resistance in malaria causing parasites imposes the need for the discovery of new potential antimalarial molecules either from natural sources or by synthesis [1]. Haem detoxification is an important biochemical process for the survival of malarial parasite [2]. Drug discovery methods that focus on the inhibition of haem detoxification can identify antimalarials, which are both potent and likely to remain useful for a longer period of time [3]. One excellent example relates to quinoline antimalarials, which acts by interfering with the haem detoxification, allowing the intraparasitic build-up of toxic haem [4]. This has defined inhibition of haem detoxification as an attractive target for designing new antimalarial drugs [5].

Discovery and development of novel antimalarials with better activities targeting haem detoxification pathway will require an understanding of both the structural and the functional characteristics (pharmacophoric features) of the known potential antimalarial molecules. Pharmacophore modeling is a drug-designing tool, which exploits the wealth of information available, including the structural and biological activity data of known active molecules. A pharmacophore model represents the three-dimensional (3D) arrangements of chemical features in a molecule that may be important for its bioactivity [6]. Qualified pharmacophore models may be used as a query for searching chemical databases to find new chemical entities. Kurosawa et al. have described the use of a 3D pharmacophore model as a query for virtual screening of database to discover antimalarial molecules [7]. Besides the application as query for database searching, 3D pharmacophore models may be used for predicting the activity of novel molecules [8–13].

We have reported a pharmacophore based predictive model [12] to discover potential antimalarial agents targeting haem detoxification pathway, which has been developed on the basis

* Corresponding author. Tel.: +91 751 2343972; fax: +91 751 2341148.
E-mail address: mpkaushik@rediffmail.com (M.Parshad Kaushik).

0223-5234/$ - see front matter © 2008 Elsevier Masson SAS. All rights reserved.
doi:10.1016/j.ejmech.2008.02.005

of quinoline antimalarials [4]. In the present study we report on the development of a pharmacophore model from structurally diversified molecules with similar mode of action, i.e. inhibition of haem detoxification process of malarial parasites. The molecules were taken from literature [4,14–21] along with their antimalarial activities against chloroquine resistant (K1) strain of malarial parasite *Plasmodium falciparum*. Number of training set molecules and input pharmacophoric features were optimized to develop a quantitative model having good correlation between actual and predicted biological activities. The optimized model was validated by Fischer's randomization test at 95% confidence level. These models were further evaluated as an activity prediction model by estimating the antimalarial activities of a test set consisting of 44 molecules taken from literature [4,14–21]. The best model was used to screen our in-house database and a compound nicotinic acid [*trans*-3-(4-ethoxy-3-methoxy-phenyl)-1-(4-hydroxy-phenyl)-allylidene]-hydrazide (**ALH5**) was obtained as a hit. The molecule was synthesized and evaluated against chloroquine sensitive (MRC-02) and resistant (RKL9) strains of *P. falciparum* and found comparable with chloroquine diphosphate (**CQ**).

2. Development of pharmacophore model

All modeling works were performed on a PIV @ 2 GHz computer with 1 GB RAM, Nvidia Quadro4 980XGL graphics card, running on Redhat enterprise Linux 2.1 WS. Catalyst 4.10 software [22] was used to generate pharmacophore models.

2.1. Building of database

Pharmacophore modeling requires structure and activity data of several active and inactive molecules for hypothesis generation. A particular molecule may show different activities in terms of IC_{50} values against different strains of *P. falciparum*. Hence in this work, these molecules were considered whose antiparasitic activity against **CQ** resistant K1 strain of *P. falciparum* has been reported. Structures of haem polymerization inhibitors with their antiparasitic activity against K1 strain from various medicinal chemistry as well as life science journals [4,14–21] were collected and developed as a unique database. The database comprises of 83 structurally diversified compounds with a wide range of experimental *in vitro* antimalarial activities against K1 strain of *P. falciparum*. Fig. 1 shows 39 molecules (C1–C39) and Fig. 2 shows 44 molecules (T1–T44). The molecules belong to different chemical classes such as quinolines (C28–C36 and T32–T40) [4], pyridines (C27 and T41) [4], bis-quinolines (C1, C2 and T1) [14], cryptolepines (C5–C14 and T2–T17) [15,16], acridines (C15–C20 and T18–T27) [17], phenothiazines (C21–C23 and T28–T30) [18], tetrahydro acridine diones (C3, C4 and T31) [19] and quinoxalines (C24–C26, T43 and T44) [20]. Some carbocyclic aromatic compounds having very good antimalarial activity such as C37 [4], C38, C39 and T42 [21] were also included in the database.

2.2. Selection of training set and test set molecules

Selection of training set molecules is the most important aspect of hypothesis generation. The selection followed some basic requirements, such as a minimum of 16 structurally diverse compounds must be selected to avoid any chance of correlation. The activity data should have a range of 3–4 orders of magnitude. Several active molecules were included in the training set so that they could provide critical requirement for pharmacophore generation. Several moderately active and inactive molecules were included to spread the activity range. By following the above criteria, 39 molecules (C1–C39) were chosen from the constructed database and put in the training set (Fig. 1). Here, biological activity data are represented as IC_{50} in nM for antimalarial activity against chloroquine resistant (K1) strain of *P. falciparum*. The activities against malarial parasite (in nM) have been classified somewhat arbitrarily as follows: highly active (<100), moderately active (101–1000) and poorly active (>1000). Rest of the molecules (T1–T44) were put in the test set (Fig. 2).

2.3. Generation of pharmacophore model

In the current work, HypoGen module of Catalyst was used to generate pharmacophore models from the training set molecules. The compounds were built using Catalyst 2D–3D sketcher. Conformational models of all training set molecules were generated using "best quality" conformational search option in Catalyst using a constraint of a 20 kcal mol^{-1} energy threshold above the global energy minimum and CHARMM force field parameters. A maximum of 250 conformations were generated to cover maximum conformational space. Instead of using just the lowest energy conformation of each compound, all conformational models for molecules in the training set were used in Catalyst HypoGen for pharmacophore hypothesis generation.

Five pharmacophoric features were used to generate pharmacophore hypotheses. The minimum and maximum counts for all the five features were kept 0 and 5, respectively. The values for uncertainty, minimum points and minimum subset points were kept the default values of Catalyst. The HypoGen module performs three important cost calculations in the units of bits that determine the success of any pharmacophore hypotheses. "Fixed cost", which represents the simplest model fits all data perfectly. "Null cost" represents the highest cost of a pharmacophore with no features and estimates the activity to be the mean of the activity data of the training set molecules. Its absolute value is equal to the maximum occurring error cost. A meaningful pharmacophore hypothesis may result when the difference between these two values (null cost – fixed cost) is more than at least 20. "Total cost" is the sum of three cost factors: a weight, an error and a configuration cost. The weight cost increases if the weight factor for the chemical features deviates from default value of 2. The error cost is solely dependent upon the root mean square (rms) differences between the estimated and actual activities of the training set molecules. The rms value represents the quality

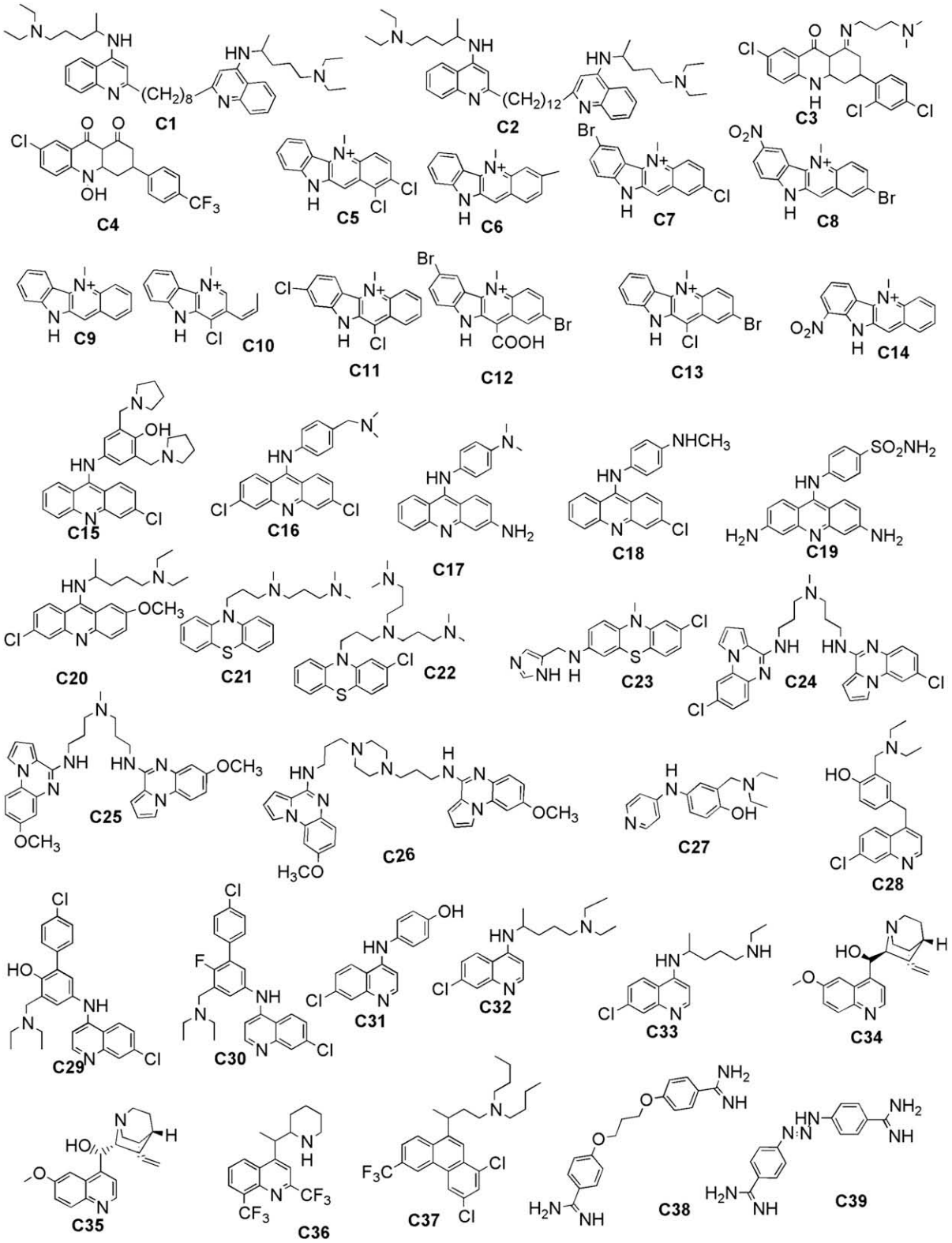

Fig. 1. Structures of 39 training set molecules.

of correlation between actual and estimated activity data. The configuration cost is represented as $\log_2 P$, where P is the number of initial hypotheses created in the constructive phase and that survived in the subtractive phase. It should not be more than 17.

2.4. Validation of pharmacophore model

To evaluate the statistical relevance of the models, Fisher's randomization test was applied. The purpose of the test is to randomize the activity data associated with the training set.

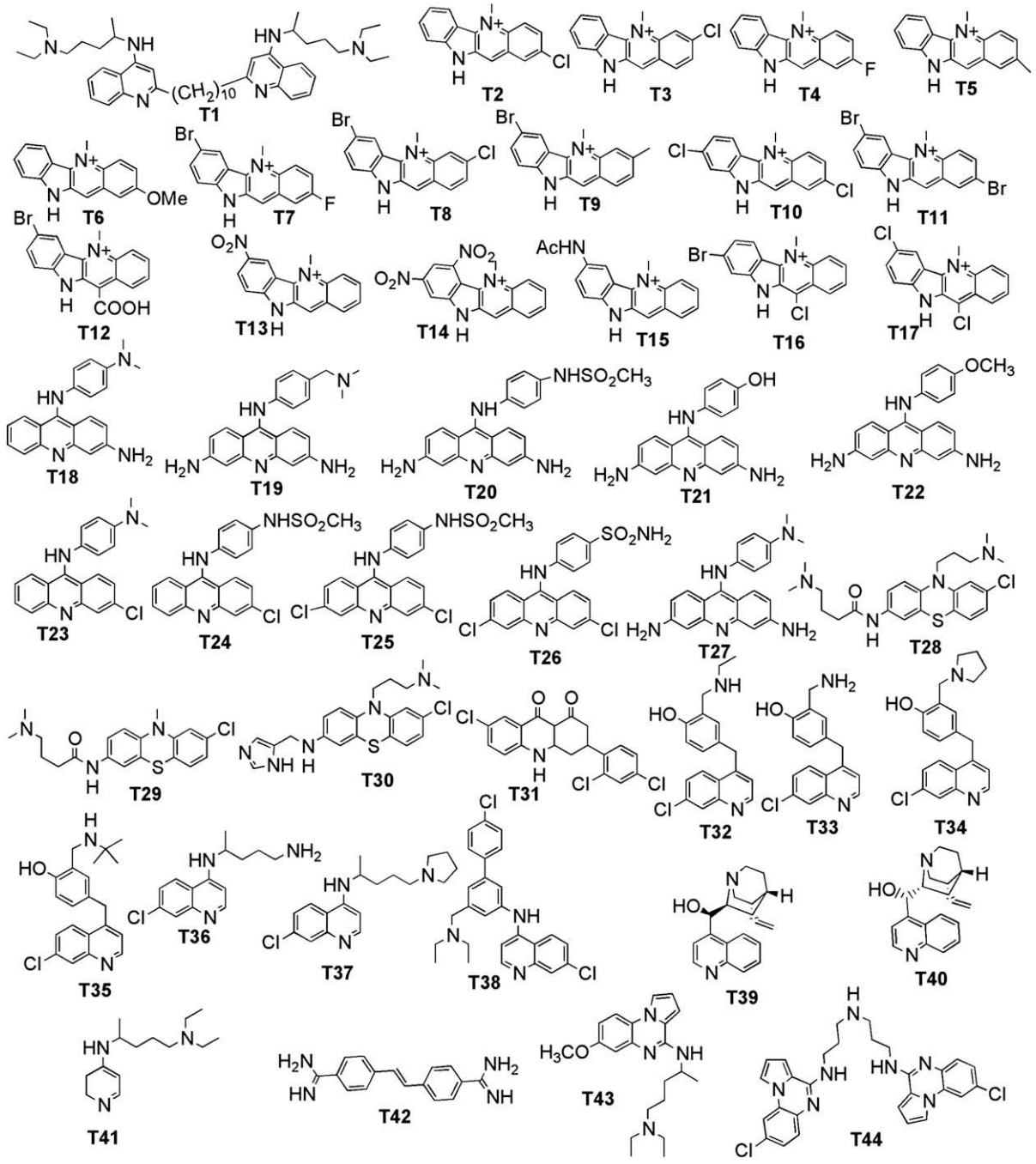

Fig. 2. Structures of 44 test set molecules.

The randomized training sets are used to generate hypotheses using the same features and parameters. If the randomized data sets result in the generation of pharmacophore with similar or better cost values, rms and correlation, then the original hypothesis is considered to have been generated by chance. The statistical significance is given by the equation of significance $= [1 - (1 + x)/y]$, where 'x' is total number of hypotheses having total cost lower than the most significant hypothesis and 'y' is the number of initial HypoGen runs + random runs. With the aid of CatScramble program available in Catalyst/HypoGen module, the experimental activities of training set molecules were scrambled randomly and resulting training sets were used for HypoGen runs. Thereby all parameters were kept as per the initial HypoGen calculation. For a 95% confidence level, CatScramble created 19 spreadsheets.

2.5. Virtual screening

A small compound library of 90 molecules was created using Catalyst 2D–3D sketcher. Conformational models of all

the molecules were generated using ''best quality'' conformational search option in Catalyst using a constraint of a 20 kcal mol^{-1} energy threshold above the global energy minimum and CHARMM force field parameters. A maximum of 250 conformations were generated to cover a broad conformational space. The library was virtually screened by a statistically valid pharmacophore model using Catalyst Compare/Fit module. The hit molecule was synthesized and analyzed against chloroquine sensitive (MRC-02) and resistant (RKL9) strains of *P. falciparum*.

3. Chemistry

Synthesis of nicotinic acid [*trans*-3-(4-ethoxy-3-methoxy-phenyl)-1-(4-hydroxy-phenyl)-allylidene]-hydrazide (**ALH5**) involved two simple steps (Scheme 1). In the first step synthesis of α,β-unsaturated ketone, *trans*-3-(3-ethoxy-4-methoxy-phenyl)-1-(4-hydroxy-phenyl)-propenone (**3**) was carried out by the well-known Claisen–Schmidt condensation reaction and the product was purified by re-crystallization from methanol. In the second step, condensation reaction between **3** and nicotinic acid hydrazide (**4**) was carried out in methanol at 65 °C. After the reaction, methanol was removed at reduced pressure and **ALH5** was purified by preparative HPLC (Knuer, Germany).

4. Antimalarial evaluation

P. falciparum strains MRC-02 (**CQ** sensitive) and RKL9 (**CQ** resistant) were obtained from National Institute of Malaria Research, New Delhi, India and maintained in a continuous culture using the standard method described by Trager and Jensen [23]. Parasites were cultured in human B (+) erythrocytes in RPMI-1640 media (GIBCO-BRL, Paisely, Scotland) supplemented with 25 mM HEPES buffer, 10% human AB (+) serum and 0.2% sodium bicarbonate (Sigma) and maintained at 5% CO_2. Cultures containing early ring stages were synchronized by addition of 5% D-sorbitol (Sigma) lysis [24], used for testing. Initial culture was maintained in small vials with 10% haematocrit, i.e. 10 μl erythrocytes containing 1.0% ring stage parasite in 100 μl complete media. The culture volume per well of the assay was 100 μl. Number of parasites for the assay was adjusted from 1% to 1.5% by diluting with fresh human B (+) RBC. Assay was done in 96-well microtitre flat-bottomed tissue culture plates incubated at 37 °C for 24 h in the presence of twofold serial dilutions of compounds and chloroquine diphosphate for their effect on schizont maturation. Compounds were dissolved in ethanol and further diluted with RPMI-1640 medium (the final ethanol concentration did not exceed 0.5% which did not affect parasite growth). Chloroquine diphosphate was dissolved in aqueous medium. Test was done in duplicate wells for each dose of the drugs. Solvent control culture containing the same concentrations of the solvent as present in the test wells was prepared with RPMI-1640 containing 10% AB (+) serum. Parasite growth was found unaffected at the solvent concentrations. Growth of the parasites from duplicate wells of each concentration was monitored by Giemsa stained blood smears by counting the number of schizonts per 100 asexual parasites. Percent schizont maturation inhibition was calculated by the formula: $(1 - N_t/N_c) \times 100$, where N_t and N_c represent the number of schizonts in the test and control wells, respectively.

5. Determination of pK_a

Acid dissociation constants (pK_as) were determined spectrophotometrically as previously described [25] by using a Unicam UV 300 spectrometer of Thermo Spectronic.

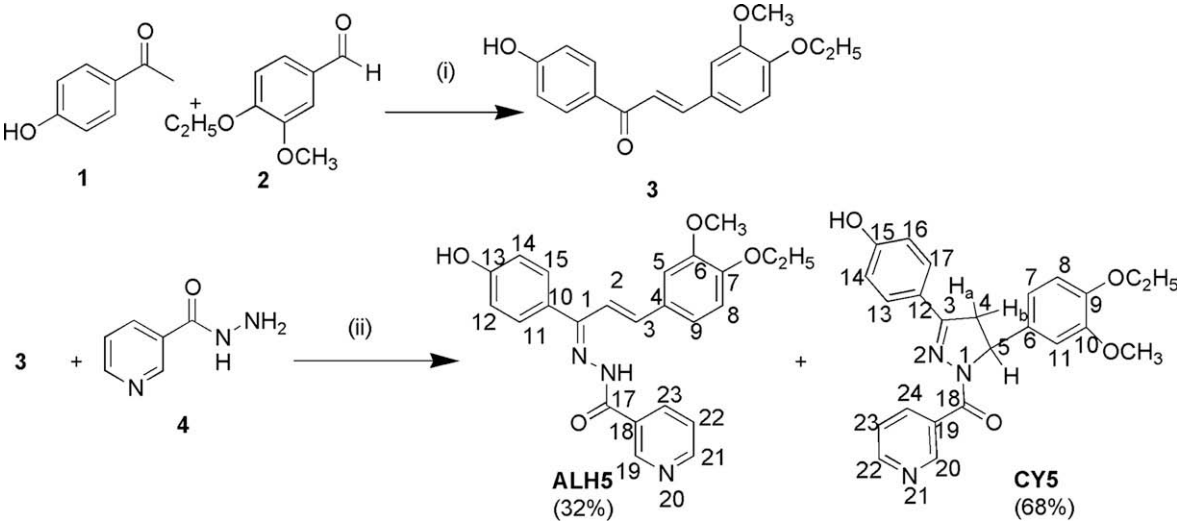

Scheme 1. Synthesis of nicotinic acid [*trans*-3-(4-ethoxy-3-methoxy phenyl)-1-(4-hydroxy-phenyl)allylidene]-hydrazide (**ALH5**). Reagents and conditions: (i) NaOMe, MeOH, r.t., 24 h; (ii) methanol, stirred for 72 h at 65 °C.

Absorbances of each compound (0.025 mg ml^{-1}) dissolved in buffers of different pH ranging from 5.8 to 11.2 as well as in 0.1 M NaOH and 0.1 M HCl were determined. Buffers from pH 5.8 to 8.0 were prepared from 0.1 M solutions of monobasic potassium phosphate (KH_2PO_4) and dibasic potassium phosphate (K_2HPO_4) and from pH 8.4 to 11.2 were prepared from 0.1 M glycine and 0.1 M NaOH. Analytical wavelengths (212 nm, 240 nm, 270 nm and 340 nm) were chosen at which significant difference between the absorbances of molecules in 0.1 M HCl and 0.1 M NaOH was observed. To reduce error, pK_a was determined in duplication at two different wavelengths for each compound.

6. β-Hematin inhibition activity

The quantitative BHIA (β-hematin inhibitory activity) assay is based on the differential solubility of hematin and β-hematin in DMSO and NaOH solution, respectively [26,27]. The method determines a 50% inhibitory concentration for β-hematin formation inhibition ($BHIA_{50}$) of the compound. In a microcentrifuge tube, 100 μl of 6.4 mM solution of hematin freshly dissolved in 0.2 N NaOH solution, 50 μl of compound dissolved in ethanol (chloroquine diphosphate was dissolved in water), 200 μl of 3 M solution sodium acetate trihydrate ($C_2H_3NaO_2 \cdot 3H_2O$), 50 μl of glacial acetic acid were incubated at 37 °C for 24 h. Concentration of compounds was varied from 6 mM to 0.3 mM range. Water and ethanol were taken as controls for water soluble and ethanol soluble compounds, respectively. Test was done in duplicates for each dose of drug. After incubation, the tubes were centrifuged for 15 min at 3300*g*. The supernatant was discarded and the pellet was reconstituted in DMSO and again centrifuged for 15 min at 3300*g*. The supernatant was discarded and β-hematin was obtained as a pellet. Following centrifugation to isolate DMSO insoluble β-hematin, the pellet was dissolved in 0.1 N NaOH and absorbance was recorded at 405 nm to calculate $BHIA_{50}$ as previously described [27].

7. Results and discussion

HypoGen develops quantitative pharmacophore hypothesis in three steps. The first step is the constructive phase, in which HypoGen identifies and stores all the possible pharmacophoric features of the active molecules. Second step is the subtractive phase, in which pharmacophoric features present in the inactive molecules are identified and subtracted from the pharmacophores stored in the constructive phase. Third step is the optimization phase in which small perturbations are applied to those features, which survived in the subtractive phase. But the quality of pharmacophoric models depends upon the input parameters like the number and diversity (structure and activity) of training set molecules and the input pharmacophoric features, which HypoGen can't decide. Hence some preliminary experiments must be carried out with HypoGen to optimize the number of training set molecules and pharmacophoric features as input parameters. Optimization was carried out in three steps. In the first step HypoGen was used for the selection of pharmacophoric features. In the second step, number of training set molecules was optimized and in the third step pharmacophoric features were optimized with respect to design the best possible models in order of their predictive ability.

7.1. Selection of pharmacophoric features

The training set molecules used for pharmacophore generation are highly diversified. By observing the structures of all the molecules, it was seen that seven pharmacophoric feature types such as hydrogen bond acceptor (HBA), hydrogen bond donor (HBD), hydrophobic aliphatic (HYALI), hydrophobic aromatic (HYAR), positive charge (PC), positive ionizable (PI) and ring aromatic (RA) could effectively map critical chemical features of all molecules in the training and test sets. But HypoGen can consider only five features at a time for hypothesis generation. Therefore eight pharmacophore models (hypo 1 to hypo 8) were generated with different combination of five input pharmacophoric features. The input and output parameters like pharmacophore features, cost values,

Table 1
Input and output parameters of pharmacophore models[a] (hypo 1 to hypo 8) generated from 39 training set molecules[b]

Model no.	Input features[c]	Output features[c]	Total cost	Fixed cost	Null cost	Conf. cost	Weight cost	rms	r[d]
hypo 1	HBA, RA, HYAR, HYALI, PI	HBA, HYALI, PI, RA	196.210	148.319	240.362	16.013	1.244	1.565	0.750
hypo 2	HBA, HBD, HYAR, RA, HYALI	HBD, HYALI, HYALI, RA	197.209	149.209	240.362	16.903	1.301	1.571	0.747
hypo 3	HBD, PI, RA, HYALI, PC	HBD, HYALI, PC, RA	195.656	148.407	240.362	16.101	1.580	1.549	0.756
hypo 4	HBA, RA, HYALI, HYAR, PI	HBA, HYALI, RA	199.122	148.561	240.362	16.255	1.422	1.605	0.734
hypo 5	HYAR, PC, RA, PI, HYALI	HYALI, PI, RA, RA	196.501	147.457	240.362	15.151	1.824	1.574	0.746
hypo 6	HBD, PI, RA, HYALI, PC	HBD, RA HYALI, PI	192.366	146.914	240.362	14.635	1.911	1.513	0.769
hypo 7	HBA, HBD, HYALI, PI, RA	HBD, HYALI, PI, RA	185.862	148.319	240.362	16.013	1.417	1.382	0.811
hypo 8	HBA, HBD, HYAR, PI, RA	HBD, PI, RA	193.575	145.277	240.362	12.971	1.128	1.573	0.746

[a] Null cost = 240.362 for all models.
[b] Molecules present in Fig. 1.
[c] HBA, hydrogen bond acceptor; HYAR, hydrophobic aromatic; HYALI, hydrophobic aliphatic; PI, positive ionizable; RA, ring aromatic; HBD, hydrogen bond donor; PC, positive charge.
[d] Correlation coefficient. All costs are in bits.

root mean square deviations (rms) and correlation coefficients (r) are listed in Table 1.

The fixed cost values of the above eight hypotheses were found close to each other because all the models were generated from same training set molecules. The weight cost and configuration cost of all the molecules were within the permissible limits. The pharmacophoric features returned in hypo 7 (Table 1) were HBD, HYALI, PI and RA with 'rms' and 'r' values of 1.382 and 0.811, respectively. For other models the above two values were found lower than hypo 7. HypoGen returned RA and PI features in all the models. HBD was returned in all the five models (hypo 2, 3, 6–8) where it was given as an input parameter. HYALI was returned in four out of five models and HBA was returned in two out of four models. HYAR and PC features were not returned in any of the models. Hence further developments of pharmacophore models were carried out with HBA, HBD, HYALI, PI and RA as input features.

7.2. Optimization of training set

Correlation coefficient signifies the closeness of the predicted biological activity with the actual activity. The better the prediction the closer is the 'r' value to 1. For hypo 7, the 'r' value was 0.811. By studying the HypoGen output file of hypo 7, 11 molecules (C1, C2, C7–C9, C11, C12, C19, C23 and C33) in the training set were found out whose predicted activities by hypo 7 were deviating >5 times from their actual values. C1 and C2 were deviating 5–7.5 times of their actual activities. C8 and C9 were found deviating between 7.5 and 10 times and others >10 times of their actual activities. In order to improve the 'r' value, some of the molecules were dropped from the training set and five models (hypo 9–13) were generated. The input pharmacophoric features were kept HBA, HBD, HYALI, PI and RA which have been optimized in the previous section. The dropped molecules, output pharmacophoric features, cost values, root mean square deviations (rms) and correlation coefficients (r) are listed in Table 2. Model hypo 12 showed $r = 0.900$, which is the best among the five hypotheses. The output pharmacophoric features of hypo 9–13 were without HBA. Hence hypo 14–18 were generated without giving HBA in the input features. But no significant improvement in correlation was observed. From this set of experiments it was observed that the training set (Fig. 1 without C7, C11, C12, C19, C23 and C33 molecules) can give a quantitative model with maximum ability of antimalarial activity prediction.

7.3. Optimization of pharmacophoric features

In the previous section, 10 models (hypo 9–18) were generated containing either three or four pharmacophoric features (Table 2). The most predictive hypo 12 was a four featured model. But five features were given to HypoGen in the input parameters to generate all the hypotheses. Hence another five models (hypo 19–23) were generated by giving four features in input parameters to find out the pharmacophoric features which can map the optimized training set molecules effectively. The input and output parameters of hypo 19–23 are listed in Table 3. It was observed that when any of the features from RA (hypo 22), PI (hypo 19) and HYALI (hypo 23) was dropped, the correlation coefficient was found below 0.9. The reason may be, without any of the above three features, the model generated could not map the training set molecules effectively and leading to wrong activity prediction. Hence RA, PI and HYALI are the three most essential features. Between the rest two features HBA and HBD, the latter was preferred by HypoGen, which can be clearly observed in the case of hypo 19. Hence HBD, HYALI, PI and RA are the four important pharmacophoric features, which can map the optimized training set molecules (Fig. 1 without C7, C11, C12, C19, C23 and C33 molecules) effectively. After optimization hypo 21 was found showing best correlation (0.906) between

Table 2
Input and output parameters of pharmacophore models (hypo 9 to hypo 18)

Model no.	Molecules dropped from the training set[a]	Output features[b]	Total cost	Fixed cost	Null cost	Conf. cost	Weight cost	rms	r[c]
hypo 9	C1, C2	HBD, PI, RA	186.005	137.890	228.812	12.311	1.131	1.612	0.734
hypo 10	C8, C9	HBD, HYALI, PI, RA	172.274	141.592	200.310	16.013	1.847	1.272	0.778
hypo 11	C7, C11, C12, C19, C23	HBD, HYALI, PI, RA	148.817	130.124	201.054	14.363	1.881	1.027	0.890
hypo 12	C7, C11, C12, C19, C23, C33	HBD, HYALI, PI, RA	143.869	128.137	197.976	16.013	1.532	0.963	0.900
hypo 13	C1, C2, C7, C8, C9, C11, C12, C19, C23, C33	HBD, HYALI, PI, RA	135.605	120.033	156.109	14.636	2.096	0.970	0.848
hypo 14	C1, C2	HBD, PI, RA	185.973	138.816	228.812	13.238	1.620	1.587	0.744
hypo 15	C8, C9	HBD, HYALI, RA	206.760	138.532	200.310	12.953	2.301	1.903	0.598
hypo 16	C7, C11, C12, C19, C23	HBD, HYALI, PI, RA	155.338	131.501	201.054	16.013	1.837	1.165	0.856
hypo 17	C7, C11, C12, C19, C23, C33	HBD, HYALI, HYALI, PI	161.656	132.392	197.976	16.904	1.174	1.310	0.901
hypo 18	C1, C2, C7, C8, C9, C11, C12, C19, C23, C33	HBD, HYALI, PI, RA	144.171	127.337	156.109	15.212	1.626	0.994	0.804

[a] Molecules present in Fig. 1.
[b] HBD, hydrogen bond donor; HBA, hydrogen bond acceptor; PI, positive ionizable; RA, ring aromatic; HYALI, hydrophobic aliphatic.
[c] Correlation coefficient. All costs are in bits.

Table 3
Input and output parameters of pharmacophore models (hypo 19 to hypo 22) with modified training set[a]

Model no.	Input features[b]	Output features[b]	Total cost	Fixed cost	Conf. cost	Weight cost	rms	r[c]
hypo 19	HBA, HBD, HYALI, RA	HBD, HYALI, RA, RA	142.002	123.175	11.051	1.392	1.067	0.885
hypo 20	HBA, HYALI, PI, RA	HYALI, PI, RA, RA	135.541	123.175	11.051	1.133	0.865	0.826
hypo 21	HBD, HYALI, PI, RA	HBD, HYALI, PI, RA	142.255	126.760	14.636	1.129	0.968	0.906
hypo 22	HBA, HBD, HYALI, PI	HBD, HYALI, HYALI, PI	148.497	128.227	16.103	1.130	1.108	0.875
hypo 23	HBA, HBD, PI, RA	HBD, PI, RA	144.246	124.198	12.073	1.238	1.099	0.878

[a] Molecules present in Fig. 1 except C7, C11, C12, C19, C23 and C33.
[b] HBD, hydrogen bond donor; HBA, hydrogen bond acceptor; PI, positive ionizable; RA, ring aromatic; HYALI, hydrophobic aliphatic.
[c] Correlation coefficient. Null cost is 197.976 for hypo 19–23. All costs are in bits.

actual and predicted antimalarial activities of training set molecules.

7.4. Validation of pharmacophore model

Fig. 3 shows regression between actual and estimated activities of the 33 training set molecules. Table 4 shows the actual and estimated activities of training set molecules in which 24 molecules out of 33 molecules were predicted correctly. All the highly active molecules ($IC_{50} < 100$ nM) were predicted correctly. Two moderately active molecules ($101\ \text{nM} < IC_{50} < 1000\ \text{nM}$) were predicted as inactive while four inactive molecules were predicted as moderately active. CatScramble was used to carry out Fisher's randomization test. The statistical validity of hypo 21 was tested at 95% confidence limit. In return pharmacophore hypotheses were generated on the basis of 19 scrambled spreadsheets. The results of CatScramble run are shown in Table 5. The data clearly show that none of the generated hypotheses after randomization had a cost value better than hypo 21. This confirmed the statistical validity of the model.

7.5. Activity prediction of test set molecules

The purpose of the hypotheses is not just to predict the activity of the training set molecules accurately but also to predict the activity of the test set molecules and classify them correctly as active or inactive. The actual and predicted activities of 44 test set molecules are given in Table 6. Most of the highly active molecules (17 out of 18) were predicted correctly. In the case of moderately active molecules 8 out of 14 were predicted correctly. T26, which is a moderately

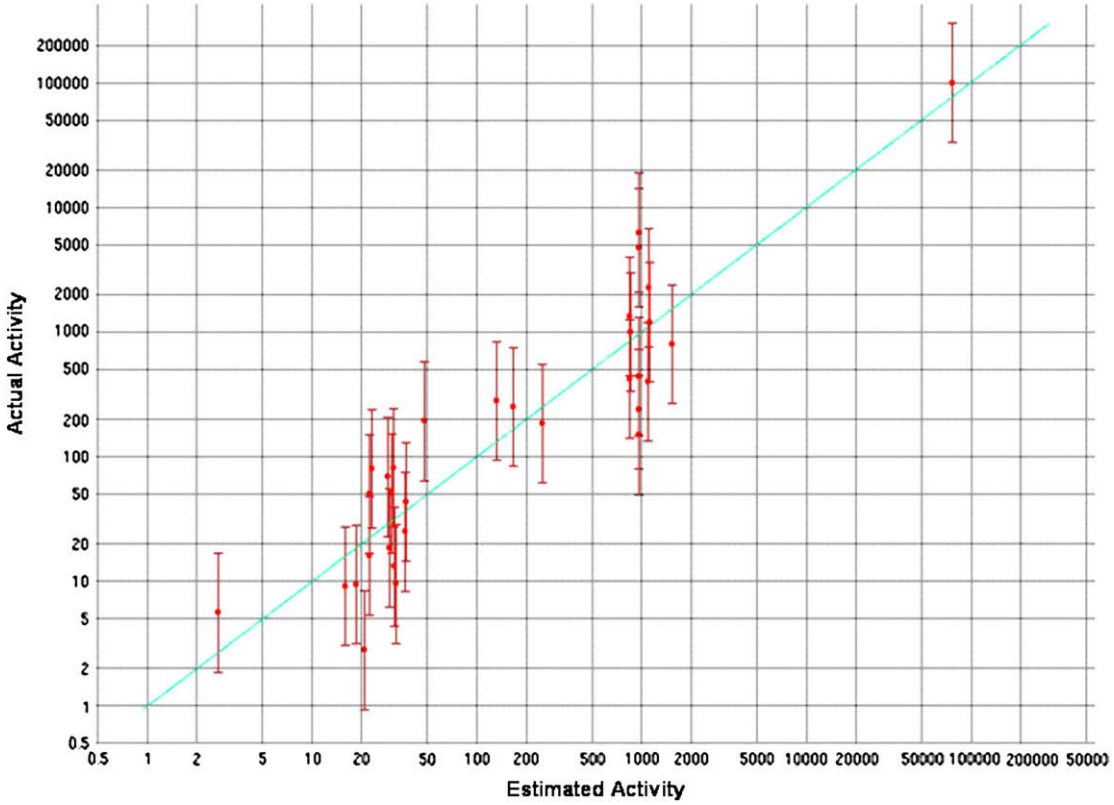

Fig. 3. Correlation ($r = 0.906$) of actual vs predicted activities by hypo 21 for the training set molecules.

Table 4
Actual and estimated activities of training set molecules calculated on the basis of hypo 21

Sl no	Code	Fit	IC_{50}[a] (nM)		Activity scale[b]		Error	References
			Actual	Estimated	Actual	Estimated		
1	C37	5.85	2.8	9.1	+++	+++	+3.3	[4]
2	C38	5.38	5.6	27	+++	+++	+4.8	[21]
3	C15	5.79	9.1	11	+++	+++	+1.2	[4]
4	C36	5.50	9.4	21	+++	+++	+2.2	[4]
5	C3	5.69	9.5	13	+++	+++	+1.4	[19]
6	C29	5.24	13	37	+++	+++	+2.9	[4]
7	C2	5.31	16	31	+++	+++	+2	[14]
8	C28	5.15	18	45	+++	+++	+2.4	[4]
9	C1	5.48	25	21	+++	+++	−1.2	[14]
10	C20	5.47	43	22	+++	+++	−2	[4]
11	C25	5.71	50	12	+++	+++	−4	[20]
12	C35	5.55	51	18	+++	+++	−2.8	[4]
13	C30	5.19	69	42	+++	+++	−1.6	[4]
14	C26	5.80	80	10	+++	+++	−7.8	[20]
15	C34	4.79	81	100	+++	+++	+1.3	[4]
16	C6	3.75	150	1100	++	+	+7.7	[15]
17	C39	3.82	190	960	++	++	+5.2	[21]
18	C32	5.37	190	280	++	++	+1.5	[4]
19	C10	3.85	240	880	++	++	+3.7	[16]
20	C16	4.50	250	210	++	++	−1.2	[17]
21	C24	4.18	280	420	++	++	+1.5	[20]
22	C4	3.83	400	950	++	++	+2.4	[19]
23	C22	3.94	420	730	++	++	+1.7	[18]
24	C5	3.75	440	1100	++	+	+2.6	[15]
25	C17	3.85	800	900	++	++	+1.1	[17]
26	C21	3.94	1000	740	+	++	−1.4	[18]
27	C18	3.87	1200	870	+	++	−1.4	[17]
28	C27	3.91	1300	780	+	++	−1.7	[4]
29	C31	3.75	2300	1100	+	+	−2	[4]
30	C13	3.85	4700	880	+	++	−5.4	[16]
31	C14	3.75	6300	1100	+	+	−5.5	[16]
32	C8	2.13	100 000	48 000	+	+	−2.1	[15]
33	C9	2.15	100 000	45 000	+	+	−2.2	[15]

[a] Data for activities for chloroquine resistant (K1) strain of *P. falciparum* are from Refs. [4,14–21].
[b] Activity scale: +++ (0–100 nM, highly active), ++ (101–1000 nM, moderately active), + (>1000 nM, poorly active).

active compound, was predicted highly active and rest five moderately active molecules were predicted inactive. For inactive molecules four were predicted correctly. Rest six molecules were predicted moderately active. Overall 29 out of 44 molecules (65%) of the test set were predicted correctly. The crossover in predictability was found mostly between moderately active and inactive molecules rather than between active to moderately active or active to inactive molecules. Hence this model may be used as a tool for new antimalarial discovery targeting haem detoxification pathway.

7.6. Virtual screening and pharmacophore mapping

Pharmacophore model hypo 21 was used as a virtual screening tool for our in-house compound library and compound **ALH5** (nicotinic acid [*trans*-3-(4-ethoxy-3-methoxy-phenyl)-1-(4-hydroxy-phenyl)-allylidene]-hydrazide) was obtained as a hit with estimated activity of 160 nM (moderately active). The two-dimensional (2D) and three-dimensional (3D) pharmacophore mappings of **ALH5** are shown in Fig. 4. Three out of four features of hypo 21 were found fitting well with **ALH5**. The only feature, which was not mapping was PI and due to this **ALH5** was predicted as moderately active.

7.7. Synthesis and antimalarial evaluation

According to our literature survey, no report has been appeared dealing with the synthesis and antimalarial evaluation of **ALH5** or similar molecules. Recently Posner et al. have reported on a novel artemisinin derivative [28] which contains nicotinic acid hydrazide side chain like **ALH5**. Hence the compound was synthesized and evaluated against malaria parasite. Synthesis of **ALH5** was carried out by condensing α,β-unsaturated ketone with nicotinic acid hydrazide. Condensation between α,β-unsaturated ketone and hydrazides are well reported in literature [29]. In the presence of acid or base or at higher temperature the reaction didn't stop after condensation but proceeds for cyclization by formation of bond between nitrogen and β-carbon. Hence substituted pyrazole

Table 5
Results from cross-validation run using CatScramble for hypo 21

Hypothesis no.	Total cost	Fixed cost	Conf. cost	Weight cost	rms	Correlation coefficient (r)
Trial 1	196.379	113.124	1.000	3.549	2.213	0.276
Trial 2	202.718	114.709	2.584	5.533	2.250	0.220
Trial 3	190.219	121.628	9.503	1.124	0.000	0.000
Trial 4	197.976	110.999	0.000	0.000	2.295	0.000
Trial 5	181.640	125.173	13.049	1.124	1.849	0.592
Trial 6	211.232	120.925	8.800	5.327	2.284	0.152
Trial 7	186.555	122.408	10.284	1.148	1.971	0.512
Trial 8	188.507	124.143	12.019	1.150	1.974	0.510
Trial 9	185.389	121.965	9.840	2.238	1.943	0.537
Trial 10	183.274	124.906	12.782	1.129	1.880	0.573
Trial 11	175.321	122.807	10.683	1.418	1.779	0.632
Trial 12	184.640	122.111	9.987	1.557	1.939	0.536
Trial 13	198.522	121.171	9.047	3.708	2.128	0.380
Trial 14	191.439	120.066	7.942	1.229	2.078	0.425
Trial 15	197.976	110.999	0.000	0.000	2.295	0.000
Trial 16	190.100	121.573	9.449	1.144	2.037	0.460
Trial 17	196.238	121.251	9.126	2.287	2.115	0.392
Trial 18	196.505	121.251	9.126	2.282	2.119	0.388
Trial 19	202.253	117.294	5.169	4.915	2.217	0.272
hypo 21	142.255	126.760	14.636	1.129	0.968	0.906

Null cost = 197.976. All costs are in bits.

[5-(4-ethoxy-3-methoxy-phenyl)-3-(4-hydroxy-phenyl)-4,5-dihydro-pyrazol-1-yl]-pyridin-3-yl-methanone (**CY5**) was obtained as product. To overcome this problem, condensation was carried out at lower temperature (65 °C) for a longer period of time (72 h). The overall yield of **ALH5** was 20% after purification by preparative HPLC. **ALH5** and **CY5** are isomers and were easily differentiated by ^{1}H NMR spectroscopy. **CY5** showed characteristic double doublet (dd) pattern at δ values 3.14 ppm (H_{4a}), 3.85 ppm (H_{4b}) and 5.67 ppm (H_5). **ALH5** did not show above pattern in the ^{1}H NMR, which confirmed the non-cyclic structure. In deuterium exchange NMR, two protons of **ALH5** at δ values 9.857 ppm and 11.366 ppm were found exchanged. This observation further validated the formation of **ALH5**.

ALH5 was evaluated against both **CQ** sensitive (MRC-02) and **CQ** resistant (RKL9) strains of *P. falciparum*. The results are shown in Table 7. Vacuolar accumulation ratios (VARs) of **ALH5** and chloroquine diphosphate (**CQ**) were theoretically calculated from experimentally determined pK_a values using Eq. (1) [30]. In Eq. (1), VAR represents the ratio of drug inside and outside of the parasite food vacuole. pH_v = pH inside food vacuole (assumed to be pH 5.5) and pH_e = pH externally (assumed to be pH 7.4).

$$\mathrm{VAR} = \frac{Q_v}{Q_e} = \left\{ \frac{1 + \dfrac{[H^+]_v}{K_{a2}} + \dfrac{[H^+]_v^2}{K_{a1}K_{a2}}}{1 + \dfrac{[H^+]_e}{K_{a2}} + \dfrac{[H^+]_e^2}{K_{a1}K_{a2}}} \right\} \quad (1)$$

ALH5 might have three pK_a values. pK_{a1} and pK_{a2} due to exchangeable protons of hydrazone moiety and phenolic hydroxyl group, respectively, have been confirmed in deuterium exchange proton NMR. The third pK_a for protonable nitrogen of pyridine might have value below 5 [31]. Its contribution for VAR would be negligible and hence not determined in the current study. The two pK_a values of **CQ** were determined

Table 6
Actual and estimated activities of test set molecules estimated by hypo 21

Code	Activity		Error	References	Code	Activity		Error	References
	Actual	Estimated				Actual	Estimated		
T1	17	34	2	[14]	T23	1100	900	−1.2	[17]
T2	166	1200	7	[15]	T24	1000	860	−1.2	[17]
T3	448	1200	2.6	[15]	T25	350	800	2.3	[17]
T4	1210	1200	−1	[15]	T26	620	65	−9.5	[17]
T5	419	120	−3.5	[15]	T27	34	86	2.5	[17]
T6	950	870	−1.1	[15]	T28	2000	590	−3.4	[18]
T7	63	100	1.6	[15]	T29	7000	4100	−1.7	[18]
T8	37	100	2.8	[15]	T30	1800	740	−2.4	[18]
T9	260	1000	3.9	[15]	T31	16	12	−1.4	[19]
T10	45	120	2.6	[15]	T32	38.8	42	1.1	[4]
T11	49	100	2	[15]	T33	166	45	−3.7	[4]
T12	260	1000	3.9	[16]	T34	11.5	44	3.8	[4]
T13	650	1100	1.8	[16]	T35	9.1	39	4.3	[4]
T14	650	1200	1.8	[16]	T36	1338	200	−6.7	[4]
T15	520	1200	2.2	[16]	T37	89.6	26	−3.4	[4]
T16	7180	2000	−3.6	[16]	T38	69.3	33	−2.1	[4]
T17	7620	880	−8.6	[16]	T39	56.2	76	1.4	[4]
T18	350	900	2.6	[17]	T40	90.6	87	1.1	[4]
T19	40	80	2	[17]	T41	15 119	7500	−2	[4]
T20	30	25	−1.2	[17]	T42	27	18	−1.5	[21]
T21	50	75	1.5	[17]	T43	1780	790	−2.3	[20]
T22	150	810	5.4	[17]	T44	790	150	−5.3	[20]

Activity scale: 0–100 nM, highly active; 101–1000 nM, moderately active; >1000 nM, poorly active.

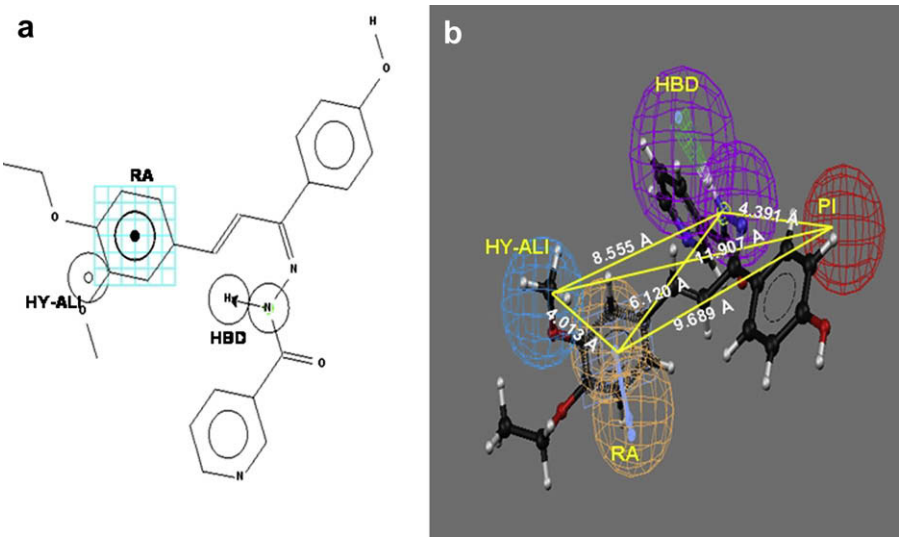

Fig. 4. Pharmacophore mapping of **ALH5** with hypo 21. (a) Two-dimensional mapping. (b) Three-dimensional mapping; the blue contour represents the HYALI feature, the orange contour represents AR feature, the magenta contour represents HBD feature and the red contour represents PI feature. Distances between features are in angstrom unit. (For interpretation of the references to colour in this figure legend, the reader is referred to the web version of this article.)

experimentally and were found close to the previously reported values [30]. The VAR and $BHIA_{50}$ values of **ALH5** were found lower than **CQ**. Due to this **CQ** was showing better antimalarial activity against chloroquine sensitive MRC-02 strain. But in the case of resistant strain, the actual VAR of **CQ** is much lower than the calculated value of Eq. (1). As RKL9 is not resistant to **ALH5**, its VAR would be comparable with the VAR of sensitive strain. Hence activity of **ALH5** was found better than **CQ** in the case of resistant strain RKL9. Activity against RKL9 strain was found closer to the estimated value by pharmacophore model hypo 21, which further validated the practical applicability of the model to discover new antimalarial compound targeting haem detoxification pathway.

8. Conclusion

In this work, we have demonstrated the generation and application of pharmacophore model (hypo 21) to discover potential antimalarial agent **ALH5**. A quantitative pharmacophore model was generated and validated targeting haem detoxification pathway of *P. falciparum*. The number of training set molecules and pharmacophoric features were optimized through a series of pharmacophore hypothesis generation. The statistically valid model was used as a virtual screening tool to discover a novel antimalarial agent nicotinic acid [*trans*-3-(4-ethoxy-3-methoxyphenyl)-1-(4-hydroxy-phenyl)-allylidene]-hydrazide (**ALH5**). The molecule was synthesized and evaluated against malarial parasite *P. falciparum*. It showed better activity than chloroquine against **CQ** resistant (RKL9) strain of *P. falciparum*. SAR studies of this class of compounds are in progress and will be communicated separately.

9. Experimental protocol

9.1. Chemistry

Nicotinic acid hydrazide, 2-hydroxy acetophenone and 3-ethoxy-4-methoxy benzaldehyde were obtained from Sigma–Aldrich. Mass spectra were acquired on a Micromass Q-ToF high-resolution mass spectrometer equipped with electrospray ionization (ESI) on Masslynx 4.0 data acquisition

Table 7
In vitro antiplasmodial activities of nicotinic acid [*trans*-3-(4-ethoxy-3-methoxyphenyl)-1-(4-hydroxy-phenyl)-allylidene]-hydrazide (**ALH5**) and chloroquine diphosphate (**CQ**)

Compound	Predicted antimalarial activity[a] (nM)	Activity vs MRC-02 strain[b] (nM)	Activity vs RKL9 strain[c] (nM)	pK_{a2}, pK_{a1}	VAR[d]	$BHIA_{50}$[e] (mM)
ALH5	160	75 ± 35	129 ± 12	9.05, 6.87	1472.04	2.35 ± 0.016
CQ	280	21 ± 3	177 ± 4	9.61, 8.55	5889.85	1.89 ± 0.009

[a] Predicted activity by pharmacophore model (hypo 21) against chloroquine resistant (K1) strain of *P. falciparum*, IC_{50}, nM.
[b] Antiplasmodial activity against chloroquine sensitive (MRC-02) strain of *P. falciparum*, IC_{50}, nM ± SD, results of two separate determinations.
[c] Antiplasmodial activity against chloroquine resistant (RKL9) strain of *P. falciparum*, IC_{50}, nM ± SD, results of two separate determinations.
[d] Vacuolar accumulation ratio (VAR) calculated using Eq. (1) and assuming vacuolar pH of 5.5 and external pH of 7.4.
[e] β-Hematin inhibitory activity, $BHIA_{50}$, mM ± SD, results of two separate determinations.

system. ESI was used in +ve ionization mode. Vibrational spectra were recorded on a Bruker Tensor 27 FTIR spectrometer. ^{1}H NMR spectra were acquired on a Bruker DPX 400 FT NMR spectrometer at 400 MHz. ^{13}C NMR spectra were acquired on Bruker AV 400 FT NMR at 100 MHz. All the NMR spectra were acquired in DMSO-d_6 at 27 °C. To check the purity, liquid chromatography–mass spectrometry (LC–ESI-MS) was carried out for all the molecules with Waters-Micromass LC-ESI-MS system equipped with Waters 1525 binary gradient pump and Micromass Q-ToF micromass spectrometer, ionized by +ve ESI mode (capillary 3000 V, sample cone 30 V, extraction cone 1 V). Separations were carried out on Waters Exterra™ C8 MS column (2.1 × 30 mm, 3.5 μ) with binary linear gradient of 5% methanol in water to 100% methanol in 20 min.

*9.2. Procedure for synthesis of nicotinic acid [trans-3-(4-ethoxy-3-methoxy-phenyl)-1-(4-hydroxy-phenyl)-allylidene]-hydrazide (**ALH5**) and [5-(4-ethoxy-3-methoxy-phenyl)-3-(4-hydroxy-phenyl)-4,5-dihydro-pyrazol-1-yl]-pyridin-3-yl-methanone (**CY5**)*

To a solution of 10 mmol (1360 mg) of 4-hydroxy acetophenone (**1**) in 10 ml methanol kept in an ice bath, 30 ml of 2 N methanolic NaOH solution was added followed by 10 mmol (1800 mg) of 4-ethoxy-3-methoxy benzaldehyde (**2**) in 10 ml methanol. The reaction mixture was stirred at 30 °C for 24 h and neutralized with hydrochloric acid. *trans*-3-(4-Ethoxy-3-methoxy-phenyl)-1-(4-hydroxy-phenyl)-propenone (**3**) appeared as a light yellow precipitate was separated by filtration and re-crystallized from methanol (2050 mg, 65% yield). Equal amount of **3** (4 mmol, 1192 mg) and **4** (nicotinic acid hydrazide, 4 mmol, 548 mg) was stirred in methanol (10 ml) at 65 °C for 72 h. Preparative HPLC was run to separate and purify the products. **ALH5** (353 mg, 20% yield), yellow amorphous solid; mp: 94–96 °C; LC–MS R_t (min): 10.73; ESI-MS (M + H): $C_{24}H_{24}N_3O_4$, 418.1667 (calculated), 418.1785 (observed); IR (KBr, cm^{-1}): 3414 (OH), 3048 (NH), 1640 (C=O), 1601 (C=N), 1265 (C–N); ^{1}H NMR (DMSO-d_6, 400 MHz) δ/ppm: 1.31 (3H, t, $J = 6.84$, CH_3), 3.79 (3H, s, OCH_3), 4.02 (2H, q, $J = 6.8$ Hz, OCH_2), 6.75–7.49 (m, Ar, 10H), 8.24 (1H, m, 22-H), 8.71 (1H, s, 21-H), 9.04 (1H, s, 19-H), 9.93 (1H, s, OH), 11.39 (1H, s, CONH); ^{13}C NMR (DMSO-d_6, 100 MHz) δ/ppm: 14.72, 55.75, 63.79, 111.29, 112.57, 115.07, 115.15, 116.19, 117.58, 121.49, 123.43, 128.11, 128.89, 130.09, 130.59, 135.88, 140.08, 149.01, 149.38, 151.91, 157.19, 158.66, 158.90, 162.81. **CY5** (750 mg, 43% yield), bright yellow crystalline solid; mp: 98–100 °C; LC–MS R_t (min): 11.78; ESI-MS (M + H): $C_{24}H_{24}N_3O_4$, 417.1667 (calculated), 418.2295 (observed); IR (KBr, cm^{-1}): 3066, 2977, 1595 (C=O), 1515, 1442, 1258, 1138, 1029, 836; ^{1}H NMR (DMSO-d_6, 400 MHz) δ/ppm: 1.30 (3H, t, $J = 6.84$, CH_3), 3.14 (1H, dd, $J = 13.5$, 4.3 Hz, 4-H_a), 3.75 (3H, s, OCH_3), 3.85 (1H, m, 4-H_b), 3.96 (2H, q, $J = 6.8$ Hz, OCH_2), 5.67 (1H, dd, $J = 11.2$, 4.2 Hz, 5-H), 6.82 (2H, d, $J = 8.2$ Hz, 14-*H*, 16-H), 6.78 (1H, m, 7-H), 6.89 (2H, m, 10-H, 11-H), 7.51 (1H, m, 23-H), 7.56 (2H, d, $J = 8.2$ Hz, 13-H, 17-H), 8.23 (1H, d, $J = 6.6$ Hz, 24-H), 8.72 (1H, s, 22-H), 9.03 (1H, s, 20-H), 10.03 (1H, s, OH).

Acknowledgement

We thank Dr. R. Vijayaraghavan, Director, DRDE, Gwalior for his keen interest and encouragement in the present work. We especially thank Dr. Shri Prakash and Dr. M.M Parida for their helpful advises and critical comments, Mr. Avik Mazumdar and Mr. Basant Lal for NMR analysis and Mr. A.K. Srivastava for FTIR and ESI-MS analyses.

References

[1] J. Sachs, P. Malaney, Nature 415 (2002) 680–685.
[2] D.E. Goldberg, A.F.G. Slater, Parasitol. Today 8 (1992) 280–283.
[3] R.G. Ridley, W. Hofheinz, H. Matile, C. Jaquet, A. Dorn, R. Masciadri, S. Jolidon, W.F. Richter, A. Guenzi, M.A. Girometta, H. Urwyler, W. Huber, S. Thaithong, W. Peters, Antimicrob. Agents Chemother. 40 (1996) 1846–1854.
[4] S.R. Hawley, P.G. Bray, M. Mungthin, J.D. Atkinson, P.M. O'Neill, S.A. Ward, Antimicrob. Agents Chemother. 42 (1998) 682–686.
[5] T.J. Egan, H.M. Marques, Coord. Chem. Rev. 190–192 (1999) 493–517.
[6] O.F. Guner, Pharmacophore Perception, Development and Use in Drug Design, International University Line, La Jolla, CA, 2000.
[7] Y. Kurosawa, A. Dorn, M. Kitsuji-Shirane, H. Shimada, T. Satoh, H. Matile, W. Hofheinz, R. Masciadri, M. Kansy, R.G. Ridley, Antimicrob. Agents Chemother. 44 (2000) 2638–2644.
[8] A. Palomer, J. Pascual, F. Cabre, M.L. Garcia, D.J. Mauleon, J. Med. Chem. 43 (2000) 392–400.
[9] M. Chopra, A.K. Mishra, J. Chem. Inf. Model. 45 (2005) 1934–1942.
[10] M.O. Taha, J. Zhang, K. Yu, W. Zhu, H. Jiang, Bioorg. Med. Chem. Lett. 16 (2006) 3009–3014.
[11] M.-Y. Li, K.-C. Tsai, L. Xia, Bioorg. Med. Chem. Lett. 15 (2005) 657–664.
[12] B.N. Acharya, M.P. Kaushik, Med. Chem. Res. 16 (2007) 213–229.
[13] N. Bharatham, K. Bharatham, K.W. Lee, J. Mol. Graphics Model. 25 (2007) 813–823.
[14] F. Ayad, L. Tilley, L.W. Deady, Bioorg. Med. Chem. Lett. 11 (2001) 2075–2077.
[15] O. Onyeibor, S.L. Croft, H.I. Dodson, M. Feiz-Haddad, H. Kendrick, N.J. Millington, S. Parapini, R.M. Phillips, S. Seville, S.D. Shnyder, D. Taramelli, C.W. Wright, J. Med. Chem. 48 (2005) 2701–2709.
[16] C.W. Wright, J. Addae-Kyereme, A.G. Breen, J.E. Brown, M.F. Cox, S.L. Croft, Y. Gokcek, H. Kendrick, R.M. Phillips, P.L. Pollet, J. Med. Chem. 44 (2000) 3187–3194.
[17] S. Auparakkitanon, W. Noonpakdee, R.K. Ralph, W.A. Denney, P. Wilairat, Antimicrob. Agents Chemother. 47 (2003) 3708–3712.
[18] M. Kalkanidis, N. Klonis, L. Tilley, L.W. Deady, Biochem. Pharmacol. 63 (2002) 833–842.
[19] A. Dorn, J.P. Scovill, W.Y. Ellis, H. Matile, R.G. Ridley, J.L. Vennerstrom, Am. J. Trop. Med. Hyg. 65 (2001) 19–20.
[20] J. Guillon, P. Grellier, M. Labaied, P. Sonnet, J.-M. Leger, R. Deprez-Poulain, I. Forfar-Bares, P. Dallemagne, N. Lemaitre, F. Pehoureq, J. Rochette, C. Sergheraert, C. Jarry, J. Med. Chem. 47 (2004) 1997–2009.
[21] A.M.W. Stead, P.G. Bray, I.G. Edwards, H.P. Dekoning, B.C. Elford, P.A. Stocks, S.A. Ward, Mol. Pharmacol. 59 (2001) 1298–1306.
[22] CATALYST 4.10, Accelrys Inc., San Diego, CA, 2005.<http://www.accelrys.com/>.
[23] W. Trager, J.B. Jensen, Science 193 (1976) 673–675.
[24] C. Lambros, J.P. Vanderberg, J. Parasitol. 65 (1979) 418–420.
[25] A. Albert, E.P. Serjeant, The Determination of Ionization Constants, Chapman and Hall Ltd., London, 1971, pp. 44–64.

[26] N. Basilico, E. Pagini, D. Monti, P. Olliaro, D.J. Taramelli, Antimicrob. Agents Chemother. 42 (1998) 55–60.
[27] R. Baelamans, E. Deharo, G. Bourdy, V. Munoz, C. Quenevo, M. Sauvain, H. Ginsburg, J. Ethnopharmacol. 73 (2000) 271–275.
[28] G.H. Posner, I.H. Paik, W. Chang, K. Borstnik, S. Sinishataj, A.S. Rosenthal, T.A. Shapiro, J. Med. Chem. 50 (2007) 2516–2519.
[29] J.-T. Li, X.-H. Jhang, Z.-P. Lin, Beil. J. Org. Chem. 3 (2007) 13. doi:10.1186/1860-5397-3-13.
[30] C.H. Kaschual, T.J. Egan, R. Hunter, N. Basilico, S. Parapini, D. Taramelli, E. Pasini, D. Monti, J. Med. Chem. 45 (2002) 3531–3539.
[31] A. Albert, E.P. Serjeant, The Determination of Ionization Constants, Chapman and Hall Ltd., London, 1971, pp. 94.